Shock ignition of thermonuclear fuel with high areal density

R. Betti[1,2], C.D. Zhou[1], K.S. Anderson[1], J.L. Perkins[3], A.A. Solodov[1]
[1]*Fusion Science Center for Extreme States of Matter and Fast Ignition Physics, Laboratory for Laser Energetics, also*[2] *Dept. of Mechanical Engineering & Physics and Astronomy, University of Rochester, Rochester, NY 14623*
[3]*Lawrence Livermore National Laboratory, Livermore, CA*

A novel method [C. Zhou and R. Betti, Bull. Am. Phys. Soc. **50**, No. 8, p. 140 (2005)] to assemble and ignite thermonuclear fuel is presented. Massive cryogenic shells are first imploded by direct laser light with a low implosion velocity and on a low adiabat leading to fuel assemblies with large areal densities. The assembled fuel is ignited from a central hot spot heated by the collision of a spherically convergent *ignitor* shock and the return shock. The resulting fuel assembly features a hot spot pressure greater than the surrounding dense fuel pressure. Such a non-isobaric assembly requires a lower energy threshold for ignition than the conventional isobaric one. The ignitor shock can be launched by a spike in the laser power or by particle beams. The thermonuclear gain can be significantly larger than in conventional isobaric ignition for equal driver energy.

PACS numbers: 52.57.-z, 52.57.Bc

In direct-drive inertial confinement fusion[1,2] (ICF), a shell of cryogenic deuterium and tritium (DT) thermonuclear fuel is accelerated inward by direct laser irradiation. As the shell stagnates, the compressed fuel is ignited from a low-density central hot spot surrounded by an ultra dense shell. For ignition to occur, the alpha particle self-heating of the hot-spot must exceed all the energy losses including expansion, heat conduction and radiation losses. As pointed out in Ref. 3, much of the heat escaping the hot spot is deposited on the surrounding dense shell inner surface causing the ablation of the shell material into the hot spot. The ablated plasma entering the hot spot carries most of the energy lost by heat conduction back into the hot spot in the form of internal energy and pdV work. If ignition occurs, the resulting burn wave propagates from the hot spot throughout the dense fuel. Most of the fusion energy yield comes from this stage of the burn when the burning plasma core is confined for a brief time by its own inertia. The burn time depends on the dense fuel areal density ρR, and the burn-up fraction is approximately given[2] by $\theta \approx 1/(1+7/\rho R)$ where ρR is in g/cm^2. The peak areal density is approximately independent of the shell implosion velocity. It increases with the laser energy and decreases with the in-flight adiabat according to the simple relation[4]

$$(\rho R)_{max} \approx \frac{1.2}{\alpha_{inn}^{0.55}} \left(\frac{E_L(kJ)}{100} \right)^{0.33} \tag{1}$$

where ρR is in g/cm^2, V_I is the implosion velocity in cm/s, E_L is the UV laser energy on target, and α_{inn} is the in-flight adiabat of the inner portion of the shell. Here, the adiabat[2] is the ratio of the plasma pressure to the Fermi pressure of a degenerate electron gas. The energy gain depends on the areal density and the capsule implosion velocity $G = (1/V_i^2)\eta_h E_f/m_i \theta(\rho R)$ where $\eta_h = E_k/E_L$ is the hydrodynamic efficiency (the ratio of the shell kinetic energy to the laser energy), $E_f = 17.5$MeV is the energy of the fusion products for a DT fusion reaction and $m_i = 2.5m_H$ is the average ion mass. Using the direct-drive hydro-efficiency[4], the energy gain can be rewritten as

$$G \approx \frac{73}{I_{15}^{0.25}} \left(\frac{3 \times 10^7}{V_I} \right)^{1.25} \frac{\theta(\rho R)}{0.2} \tag{2}$$

where the laser intensity I_{15} is in units of 10^{15}W/cm^2. In deriving Eq. (2), it is assumed that ignition has taken place and the burn wave has propagated through the dense core. Notice that Eq. (2) indicates that the gain increases for lower implosion velocities since more mass can be assembled for the same laser energy. In addition to the high gains, massive shell implosions have good hydrodynamic stability properties during the acceleration phase. The number of e-folding of Rayleigh-Taylor (RT) instability growth for the most dangerous modes with $k\Delta \approx 1$ (k is the mode wave number and Δ is the in-flight target thickness) is[2,4] $\gamma t \approx 0.9\sqrt{IFAR_{max}}$ where $IFAR$ is the in-flight aspect ratio[2] that can be approximated[4] by

$$IFAR_{max} \simeq \frac{51}{< \alpha_{if} >^{0.6}} \left(\frac{V_I(cm/s)}{3 \cdot 10^7} \right)^2 \frac{1}{I_{15}^{4/15}} \tag{3}$$

where $< \alpha_{if} >$ is the average in-flight adiabat. Thus, low IFAR implosions are not significantly affected by the RT instability. However, low IFAR implosions are difficult to ignite since the energy required for conventional ignition scales approximately[4,5] as $E_{kin}^{ign} \sim IFAR^{-3}$ for a fixed laser intensity. This can be shown by substituting Eq. (3) into the well known scaling[5] of the kinetic energy required for ignition $E_{kin}^{ign} \sim \alpha^{1.9} V^{-5.8} p_L^{-0.77}$ where $p_L \sim I_L^{2/3}$ is the applied laser pressure[2]. Thus, while low-adiabat low-velocity implosions have the potential for high gains, their hot-spot energy is not enough to trigger ignition.

The conventional inertial fusion assembly of the hot spot and surrounding dense fuel is isobaric[6] with the plasma pressure approximately uniform throughout the entire core (Fig. 1). Both the low-density central hot spot and the high density cold surrounding fuel have similar internal energy densities. However, an isobaric fuel

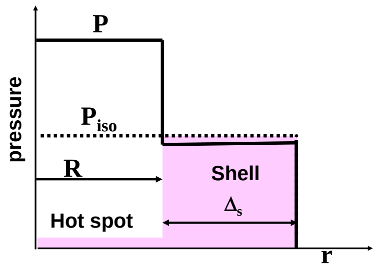

FIG. 1: Sketch of a uniform pressure *isobaric* assembly (dashed) and of a non-isobaric assembly with the pressure peak inside the hot spot (solid)

assembly is not optimal for central ignition. Here, we show that a stagnating core with a non-uniform pressure peaked inside the hot spot has a lower ignition threshold than a uniform pressure core for the same total internal energy. We also show that such a peaked pressure profile can be attained by launching a spherically converging shock in the latest stage of the implosion. The launching time of such an *ignitor* shock must be carefully chosen. In order to maximize the hot-spot peak pressure of the final assembly, the ignitor shock must collide with the return shock inside the dense shell and near its inner surface. The return shock is the outward traveling shock driven by the rapidly increasing hot spot pressure during the shell slowing down. The inward moving shock generated by the collision leads to a further compression of the hot spot and to a peaked pressure distribution. In this paper, we first show that a peaked pressure profile leads to a lower ignition threshold. Then, using a simple planar hydrodynamic model, we show that a peak pressure profile can be attained by launching a shock at the appropriate time. Finally, we use ICF hydro-codes to simulate realistic implosions with ignitor shocks.

We consider the assembly in Fig.1, and use the hot spot model of Ref. 3. We assume that heat conduction losses are fully recycled into the hot spot, and derive the ignition conditions by balancing the alpha heating with the radiation and expansion losses. The latter represent the transfer of the hot-spot internal energy into the rebounding shell kinetic energy[3,7]. The radiation losses are retained since the capsules considered here have low implosion velocities ($V_I < 3\cdot 10^7 cm/s$) leading to relatively cold hot spots ($T_{max} < 7keV$). Defining with R the hot spot radius, assuming that the pressure p is uniform within the hot spot and using the volume average operator $<>\equiv 3\int_0^1 x^2dx$ with $x = r/R$, the ignition condition can be written in the following simple form

$$P_\alpha > P_{exp} + P_{rad} \tag{4}$$

$$\frac{P_\alpha}{U} \sim p\left\langle\frac{\bar{\sigma v}}{T^2}\right\rangle,\quad \frac{P_{exp}}{U} \sim \frac{1}{\tau_{dec}},\quad \frac{P_{rad}}{U} \sim p\left\langle\frac{1}{T^{3/2}}\right\rangle, \tag{5}$$

where $U \sim pR^3$ is the internal energy, and τ_{dec} is the decompression time. Following Ref. 3, the decompression time scales as $\tau_{dec} \sim \sqrt{M_{shell}/pR}$, where M_{shell} is the shell mass. Using Eq. (2.2) of the first Ref. 2 for the radiation power density, and combining the alpha heating and the radiation losses leads to

$$P_\alpha - P_{rad} \sim p^2R^3T_0^\beta\left[1-(T_*/T_0)^{\beta+3/2}\right] \tag{6}$$

where T_0 is the central temperature for the profile[3] $T = T_0(1-x^2)^{2/7}$ and $T_* \approx 6.4$keV is the critical value of the central temperature corresponding to the balance of the alpha heating and radiation losses. If a fraction of the radiation losses is re-absorbed or recycled into the hot spot, the critical temperature T_* decreases with $T_* \approx 5$keV for a 50% recycling. The parameter β comes from the power law approximation of $\bar{\sigma v}/T^2 \sim T^\beta$. Since we are considering ignited hot spots, the parameter β is chosen to optimize the power-law fit of $\bar{\sigma v}/T^2$ for central temperatures exceeding T_*. We consider central temperatures ranging from 5 to 15keV, and approximate the volume-averaged alpha heating term $<\bar{\sigma v}/T^2>$ with a power law of the central temperature T_0^β with $\beta \simeq 1$. Substituting Eq. (6) into (4) yields the ignition condition

$$(p/R)M_{shell}T_0^2\left[1-(T_*/T_0)^{2.5}\right]^2 > const \tag{7}$$

Though Eq. (7) is valid for an arbitrary fuel assembly, it is convenient to introduce the parameters $\hat{\Phi} \equiv pR_{iso}/p_{iso}R$ and $\hat{\delta} \equiv T_0/T_0^{iso}$, where iso indicates an isobaric fuel assembly (Fig. 1). The ignition condition can be simplified by setting $M_{shell} \sim \rho_s\Delta_sR^2\Sigma$ where ρ_s and Δ_s are the shell density and thickness, and $\Sigma \equiv 1+A^{-1}+A^{-2}/3$ with $A = R/\Delta_s$. Furthermore, using the isobaric profile, we set $M_{shell}V_I^2 \sim p_{iso}R_{iso}^3(1+A^{-1})^3$, and rewrite the ignition condition in terms of the shell areal density $(\rho_s\Delta_s)^{iso}$ of the isobaric assembly

$$(\rho_s\Delta_s)^{iso} > \frac{const\left[1-\left(T_*/\hat{\delta}T_0^{iso}\right)^{2.5}\right]^{-1}}{\hat{\Phi}^{0.5}\hat{\delta}T_0^{iso}V_I\Psi(A)} \tag{8}$$

where $\Psi(A) \equiv \Sigma(A)/(1+A^{-1})^{3/2} \approx const$ for relevant values of $1 < A < 4$. The parameters $\hat{\Phi}$ and $\hat{\delta}$ represent the non-isobaric modifications of the ignition condition. If the non-isobaric assembly is achieved through an adiabatic compression of the hot spot ($p\cdot vol^{5/3} = const$), then $\hat{\delta} \sim \hat{\Phi}^{1/3}$. The scaling of the shell areal density for an isobaric assembly is given in Eq. (1), while the scaling of the central temperature is given[8] by $T_0 \sim V_I^{1.3}/\alpha^{0.06}$ yielding the following final form of the ignition condition in terms of the laser energy required for ignition

$$E_L > \frac{E_{ign}^{iso}}{\hat{\Phi}^{2.5}}\left[1-\left(\frac{V_*}{\hat{\Phi}^{0.25}V_I}\right)^{3.3}\right]^{-3} + \Delta E^{n.i.}(\hat{\Phi}) \tag{9}$$

where $E_{ign}^{iso} \sim \alpha^{1.8}/V_I^{6.9}$, is the laser energy required for high-velocity ($V_I >> V_*$) isobaric ignition, V_* is the

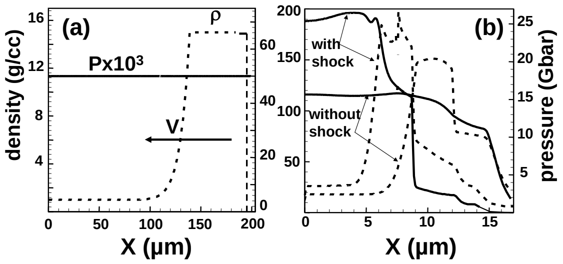

FIG. 2: Pressure (solid) and density (dashed) profiles of a plasma slab hitting a rigid wall. Figure (a) shows the initial profiles. Figure (b) shows the profiles at peak compression.

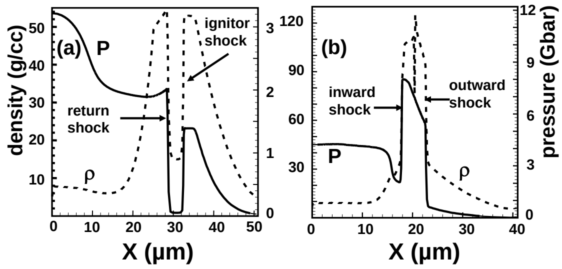

FIG. 3: Pressure (solid) and density (dashed) profiles for the plasma slab before (a) and after (b) the shocks‘ collision

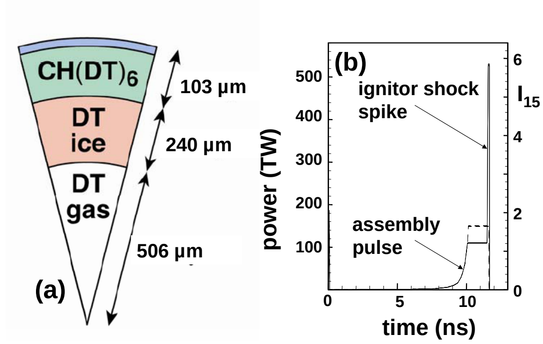

FIG. 4: Wetted-foam target (a) and 290kJ UV laser pulse (b) with (solid) and without (dashed) the shock power spike

critical implosion velocity required to achieve $T_0 = T_*$, and $\Delta E^{n.i.}(\hat{\Phi})$ is the additional laser energy required to generate the non-isobaric fuel assembly with $\hat{\Phi} > 1$. There are not accurate values for V_* and T_* but typically $T_* \sim 5$keV and $10^7 < V_* < 2 \cdot 10^7$cm/s. If $\hat{\Phi} = 1$, the fuel assembly is isobaric and $\Delta E^{n.i.} = 0$. This ignition model yields an isobaric ignition scaling similar to the one in Ref. 5. Indeed, using the hydrodynamic efficiency scaling of Ref. 4, $\eta \sim V_I^{0.75}/I^{0.25}$, the ablation pressure scaling $P \sim I^{2/3}$ and taking the limit of $V_I >> V_*$, the kinetic energy required for isobaric ignition $E_{kin}^{iso} = \eta E_{ign}^{iso} \sim \alpha^{1.8}/V_I^{6.1} p_L^{0.4}$ is remarkably close to the scaling[5] of conventional ICF implosions. If the peaked hot spot pressure in the non-isobaric assembly is achieved through an adiabatic compression, the factor $\hat{\Phi}^{2.5} \sim (p/p_{iso})^3$. Notice that the ignition energy [Eq.(9)] is lowered significantly for a moderate increase of p (for example, $\hat{\Phi}^{2.5} \approx 5$ for $p \approx 1.7 p_{iso}$). There may not be a unique approach to induce a non-isobaric assembly of the kind in Fig. 1. Here, we show that launching a shock during the final stage of the implosion, and timing it with the return shock is an attractive option to generate a non-isobaric assembly. This can be shown using a simple planar model of a plasma slab compressing a lower density plasma (Fig. 2a). The plasma is initially traveling towards a rigid wall at $x = 0$, with a constant velocity V_I and a uniform pressure of 50Mbar (Fig. 2a). The evolution is described by the single fluid Euler equations and the shock is driven by an applied pressure pulse on the plasma slab outer edge. We compare the compressed core for an initial velocity of $V_I = 2.5 \cdot 10^7 cm/s$ without a shock, and the one for an initial velocity of $V_I = 2.16 \cdot 10^7 cm/s$ with a shock. The shock-driving pulse has a pressure of 1.4Gbar for 200ps. The total energy with and without a shock is the same. The shock launching time of 320ps is chosen to maximize the peak pressure in the hot spot. Figure 2b shows the compressed cores with and without shock. The non-isobaric core has a hot spot pressure 70% larger than the isobaric core, and the energy used to drive the shock is only 23% of the total energy. It is important to observe that the driven shock (we refer to it as the *ignitor* shock) collides with the return shock inside the shell. The return shock is the outward moving shock driven by the rising pressure in the hot spot. Figure 3a shows the two shocks right before the collision. As a result of the collision, two new shocks are generated: an inward and outward moving shock (Fig. 3b). It is the inward moving shock that impulsively accelerate the inner shell surface thus enhancing the piston action of the shell on the hot spot and leading to the non-isobaric assembly of Fig. 2b.

The shock-ignition technique can be used to lower the ignition energy in inertial fusion implosions. The ignitor shock can be launched by a spike in the laser power or by a particle beam. The latter being a more efficient way to drive shocks since particle beams deliver their energy directly onto the target. Existing large laser facilities such as the National Ignition Facility[9] (NIF) should be capable of testing this concept through laser-driven shocks. As an example, we consider a massive $850\mu m$ outer radius, $343\mu m$-thick wetted-foam capsule (Fig. 4a) driven by the UV laser pulse shown in Fig. 4b. The implosion is simulated with the hydro-code LILAC[10]. The pulse shape (solid curve in Fig. 4b) consists of an adiabat-shaping[11] assembly pulse with a flat top power of $110-130$TW setting the shell on an inner adiabat $\alpha_{inn} \approx 1$, average adiabat $< \alpha_{if} >\approx 2$ and velocity $V_I \simeq 2.25 \cdot 10^7$cm/s. The $IFAR_{max} \approx 18$ is so low that the shell remains integral during the acceleration phase. The ignitor shock is driven by a spike in the laser power reaching 540TW for about

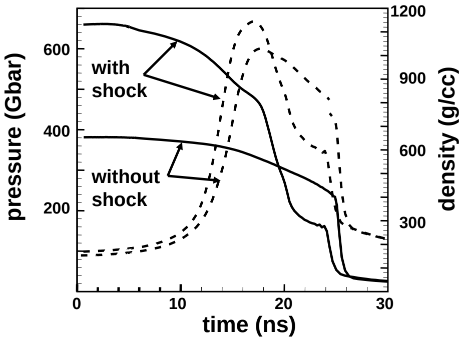

FIG. 5: Pressure (solid) and density (dashed) profiles at peak compression for the 290 kJ pulse shapes with and without ignitor shock

100-300ps. Because of the relatively high laser intensity $\sim 6\cdot 10^{15}\mathrm{W/cm}^2$ in the spike, a significant amount of hot electrons can be generated by the laser plasma instabilities. In the simulations, we let up to 10% of the spike laser energy converted into hot electrons with a temperature of 100keV. The hot electrons are transported to the target according to a multi-group diffusion model[10] and typically only a small fraction $< 10\%$ of the hot electron energy reaches the target. Since the target areal density is quickly rising at the end of the pulse, hot electrons with energy $\leq$ 100keV do not penetrate through the target but are stopped near the surface thus augmenting the drive for the ignitor shock. We find that the total laser energy for marginal shock ignition is 290kJ partitioned between the assembly pulse (243kJ) and the power spike (47kJ). The effects of the ignitor shock on the fuel assembly are shown in Fig. 5, where the pressure and density profiles at peak compression are shown for the target in Fig. 4a imploded by the shock-ignition pulse shape (solid curve in Fig. 4b) and the conventional pulse shape (dashed curve) with the same energies of 290kJ and without alpha deposition. The non-isobaric assembly has a peak pressure 70% higher than the isobaric one, corresponding to a reduction of the ignition energy (without including the ignitor shock energy) of $\hat{\Phi}^{2.5} \approx 4.9$ (see Eq. 9). Using Eq. (9), $E_L = 290\mathrm{kJ}$, $\Delta E_L^{n.i.} = 47\mathrm{kJ}$ and $\hat{\Phi}^{2.5} \approx 4.9$, we can recover the isobaric ignition energy $E_L^{iso} \simeq 1.19\mathrm{MJ}$. We verified this result by using the hydro-code LILAC to find that marginal isobaric ignition (without the shock) for the same implosion velocity, adiabat and intensity requires a 1.5mm radius target and a 1.15MJ UV laser driver. If shock-ignited with a laser energy of 310kJ (20kJ above the marginal energy), the target in Fig. 4 yields a 1D thermonuclear gain of 55 higher than the gain expected from the 1.5 MJ conventional direct[12] and indirect[9] drive on the NIF. However, one needs to be cautious in using the 1D results to assess the viability of this concept. Since the ignitor shock is launched at the end of the acceleration phase, the target nonuniformities are transferred to the shock front and carried to the hot spot by the shock. A distorted hot spot can quench[5,13] the ignition. An excess energy above the marginal ignition energy of 290kJ will be required to overcome the yield degradation due to nonuniformities. We use the 2D hydro-code DRACO[14] to simulate the implosion of the capsule in Fig 4a driven by a shock-ignition UV-laser pulse of 425kJ. The pulse has an excess energy of 135kJ with respect to the marginal 1D value. About 275kJ are used in the assembly pulse and 150kJ in the shock spike. The robustness of the ignition is assessed by the size of the ignitor-shock launching window (LW) representing the time interval during which the ignitor-shock can be launched to successfully ignite the core. In 1D, the LW is about 400ps with the gain varying from 30 for a shock launched at the early time in the LW, and 60 for a shock launched at the late time in the LW. In the 2D simulations, we include the laser nonuniformities according to direct-drive NIF-like specifications[12] for the mode numbers $l \leq 100$ relevant to such thick targets. As expected, we find that laser non-uniformities do lead to a reduction of the LW size. The LW is reduced by 170ps to 230ps with the energy gain still about 60 for a shock launched in the late time in the LW.

In summary, shock-ignition can significantly reduce the driver energy requirements to achieve high thermonuclear energy gains. The shock launched at the end of the acceleration phase of an imploding shell, can trigger ignition at relatively low driver energies by inducing a non-isobaric assembly with a peaked pressure. This work has been supported by the US Department of Energy under Cooperative Agreement ER54789 and DE-FC03-92SF19460.

[1] J. Nuckolls *et al*, Nature **239**, 139 (1972)
[2] S. Atzeni, J. Meyer-ter-Vehn *The Physics of Inertial Fusion* (Clarendon Press, Oxford, 2004); J.D. Lindl *Inertial Confinement Fusion* (Springer, New York, 1998)
[3] R. Betti *et al*, Phys. Plasmas **8**, 5257 (2001)
[4] R. Betti and C. Zhou, Phys. Plasmas **12**, 110702 (2005); R. Betti *et al*, Plasma Phys. Control. Fusion **48**, B153 (2006)
[5] M.C. Herrmann, M. Tabak, J.D. Lindl, Phys. Plasmas **8**, 2296 (2001)
[6] J. Meyer-ter-vehn, Nuc. Fusion **22**, 561 (1982)
[7] M. Basko and J. Johner, Nuc Fusion **38**, 1779 (1998);
[8] C. Zhou and R. Betti, Bull. Am. Phys. Soc. **51**, No. 7, p. 31 (2006) and submitted to Phys. Plasmas
[9] S. W. Haan *et al*, Phys. Plasmas **2**, 2480 (1995)
[10] J. Delettrez, E. B. Goldman, Laboratory for Laser Energetics Report No.36 (NTIS Document No. DOE/SF/19460/118)
[11] V. Goncharov *et al*, Phys. Plasmas **10**, 1906 (2003); K. Anderson and R. Betti, Phys. Plasmas 11, 5 (2004)
[12] P.W. McKenty, et al. Phys. Plasmas 8, 2315 (2001)
[13] R. Kishony and D. Shvarts, Phys. Plasmas **8**, 4295 (2001)
[14] P. Radha *et al*, Phys. Plasmas **12**, 032702 (2005)